Computer Science Department of The University of Auckland
CITR at Tamaki Campus (http://www.citr.auckland.ac.nz)

CITR-TR-100 September 2001

Albedo Recovery Using a Photometric Stereo Method

Chia-Yen Chen, Reinhard Klette[1] and Ramakrishna Kakarala[2]

Abstract

This paper describes a method for the calculation of surface reflectance values via photometric stereo. Experimental results show that surfaces rendered with reflectance values calculated by the proposed method have more realistic appearances than those with constant albedo.

[1] Center for Image Technology and Robotics Tamaki Campus, The University of Auckland, Auckland, New Zealand.

[2] Agilent Technologies Laboratories, Palo Alto, CA 94304, USA

Albedo Recovery Using a Photometric Stereo Method

Chia-Yen Chen, Reinhard Klette
CITR, Tamaki Campus
The University of Auckland, Auckland, New Zealand
and
Ramakrishna Kakarala
Agilent Technologies Laboratories, Palo Alto, CA 94304, USA

Abstract

This paper describes a method for the calculation of surface reflectance values via photometric stereo. Experimental results show that surfaces rendered with reflectance values calculated by the proposed method have more realistic appearances than those with constant albedo.

Keywords: surface reflectance, albedo, photometric stereo.

1 Introduction

One of the key topics addressed by the Synthetic-Natural Hybrid Coding portion of the MPEG-4 standard is the compression and simplification of synthetic data representations, including the photometry properties, such as colors, surface normals, surface properties and texture attachments [1]. The required photometry properties can either be modelled or extracted from given data. For example, the colors can be obtained using cameras, surface normals can be calculated by various shape from X methods, surface reflectance properties may be modelled using known reflectance models. Nevertheless, in many situation, synthetic modelling alone is insufficient to render realistic looking objects, particularly in the area of surface reflectance properties. Hence it is desirable to develop approaches for the attainment of various photometry properties.

Apart from the application in MPEG-4, another reason for obtaining the surface reflectance properties of various objects lies in the visualisation of the reconstructed 3D model. In many other applications, it is often necessary to render the resultant 3D model from different viewing directions and under different illumination conditions. It is imperative that the model should be rendered as close to the actual object as possible. However, usual reflectance models are

insufficient to render realistic looking objects. At this point, the result of rendering can be significantly improved if the surface reflectance properties of the original object are provided.

In this work, we propose a method for the recovery of surface reflectance, i.e., the albedo values at each given surface point, using the photometric stereo method [2, 3, 6].

PSM is firstly applied under the assumption of Lambertian reflectance to recover the surface normals. The calculated surface normals are used to extract the composite albedo from the input images of the object.

Experiments have shown that the surfaces rendered using calculated albedo have intensity values that are closer to that of the input images, i.e. the rendered results are more realistic than surfaces rendered using an assumed reflectance model.

2 Model

At each point $\mathbf{t}$ on a surface, there is a wavelength-dependent bidirectional reflectance distribution function (BRDF). The BRDF is defined to be the ratio of reflected radiance to the incident irradiance. At the point $\mathbf{t}$, the BRDF is a function of the incident light direction $\mathbf{s}$, the surface normal $\mathbf{n}$), the direction of view $\mathbf{v}$, and the wavelength λ:

$$\text{BRDF} = f_{\mathbf{t}}(\mathbf{s}, \mathbf{n}, \mathbf{v}, \lambda).$$

If the 3-D shape of the object is known (as measured from photometric stereo, for example), then $\mathbf{n}$ is determined for every $\mathbf{t}$. Generally, the illumination direction $\mathbf{s}$ and direction of view $\mathbf{v}$ are also known. It is only necessary to determine how $f_{\mathbf{t}}$ varies a function of λ. In what follows, we ignore the dependence on $\mathbf{t}$, $\mathbf{s}$, $\mathbf{v}$, and $\mathbf{n}$, and write simply $f(\lambda)$.

It is known from studies of human colour perception that reflectance functions may be accurately modelled (at least for purposes of our visual discrimination) by a low-order orthogonal basis expansion, i.e.,

$$f(\lambda) = \sum_{k=1}^{n} \alpha_k x_k(\lambda).$$

The basis functions $x_k(\cdot)$ have been determined [4]. Typically $n = 7$ gives an excellent fit to most surfaces, and even $n = 4$ is useful for many applications.

Suppose that the incident illumination is $E_\ell(\lambda)$. A colour camera has three types of sensors (usually red, green, and blue), with responses $r_j(\lambda)$, for $j = 1, 2, 3$. The response of the j-th sensor to the reflected light from illumination ℓ is

$$r_{\ell j} = \int_\lambda E_\ell(\lambda) r_j(\lambda) \sum_{k=1}^{n} \alpha_k x_k(\lambda) d\lambda.$$

We can also write

$$r_{\ell j} = \sum_{k=1}^{n} \alpha_k \int_{\lambda} E_\ell(\lambda) r_j(\lambda) x_k(\lambda) d\lambda.$$

This integral involves functions which are either known, or measured independent of the object. Hence, the integral can be calculated "off-line", resulting in the expression

$$r_{\ell j} = \sum_{k=1}^{n} \alpha_k C_{\ell j k}.$$

With L light sources, a total of $3L$ responses $r_{\ell j}$ may be measured. If $3L \geq n$, then the unknown reflectance parameters α_k are determined.

In what follows, the model is discussed for $n = 1$ (scalar), and the dependence on wavelength λ is suppressed. Therefore, we write $\rho = f(\lambda)$ to denote reflectance.

3 Calculation of albedo

The Lambertian reflectance function R for a surface Z under orthographic projection can be written as

$$\begin{aligned} R(p,q) &= \eta \, cos\theta_i + \sigma \\ &= E_0 \rho \, cos\theta_i + \sigma \end{aligned} \tag{1}$$

where $p = \frac{\delta Z}{\delta X}$ and $q = \frac{\delta Z}{\delta Y}$ are the partial derivatives of the surface Z, η is the composite albedo which combines the light source intensity E_0 and the intrinsic reflectance of the surface material ρ, θ_i is the incident angle between the surface normal and light source direction, and σ is the bias intensity due to background illumination, sensor calibration and quantization of irradiance values [5].

Assuming the Lambertian model for surface reflectance, the photometric stereo approach for surface recovery is able to calculate light source directions given a calibration object with known surface geometry (such as a sphere). From the calibrated light source directions, the photometric stereo method estimates the partial derivatives, p and q, of an object surface. An albedo independent analysis is employed because the albedo values are (initially) completely unknown for points on the surface.

In our work, three non-collinear light sources are used to illuminate the object from different directions for shape recovery using photometric stereo. The calculated surface normals are substituted into the Lambertian reflectance function to find the composite albedo η. The bias intensity is usually assumed to be zero for simplicity. Therefore, the composite albedo at position (x, y) is

$$\eta(x,y) = E(x,y)/cos\theta_i \tag{2}$$

where $E(x,y) = R(p,q)$ is the image intensity at position (x,y).

Ideally, the light source direction is constant under parallel illumination and surface points with $\theta_i > \pi/2$ will not be illuminated. However, in experimental conditions with a point light source, the illumination from the light source spreads. Also, interreflections from the surface contribute to additional illuminations. The combined effect is such that even regions with $\theta_i > \pi/2$ are illuminated, i.e. self-shadowing of the surface does not occur strictly at the $\theta_i = \pi/2$ boundary. For regions where $cos\,\theta_i < 0$, i.e. the incident angle is in the range of $(-\pi, -\pi/2)$ or $(\pi/2, \pi)$, the calculated η becomes negative. However, since E_0 nor ρ can be negative, the equation for η can be re-written as

$$\eta(x,y) \quad = |E(x,y)/cos\theta_i|\,. \tag{3}$$

For points where $cos\theta_i$ is close to 0, i.e., the surface normals are almost perpendicular with the light source direction, the values of η are more likely to be erroneous. Hence large values from such points are eliminated by a threshold operation. The threshold can be determined independently for each situation by setting it to, say the top five percentile of all the calculated η values. Values that are larger than the threshold are discarded. The remaining values of η provide an estimation of the visible surface's reflectivity.

4 Results

Following the method mentioned, values of η are calculated for each point on the visible surface of the object.

In our work, we use images obtained for PSM to estimate η for a real plaster *Beethoven* head bust from different viewing directions. There are three input images for each direction. In each image, the object is illuminated from a calibrated light source. All three images are combined to obtain the surface normals for each visible point on the surface. Once the surface normals are

Figure 1: Examples of input images.

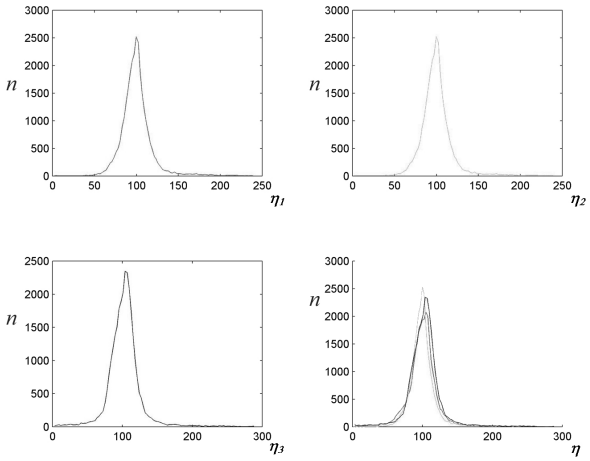

Figure 2: Distribution of calculated η values.

obtained, we calculate the η values separately for the three different light source directions.

Figure 1 shows a set of input images for light source directions $ls_1 = (0.27, -0.10, -1)$, $ls_2 = (0.01, 0.20, -1)$, and $ls_3 = (-0.26, -0.08, -1)$, respectively from left to right.

Figure 2 shows distributions of η calculated for each light source direction.

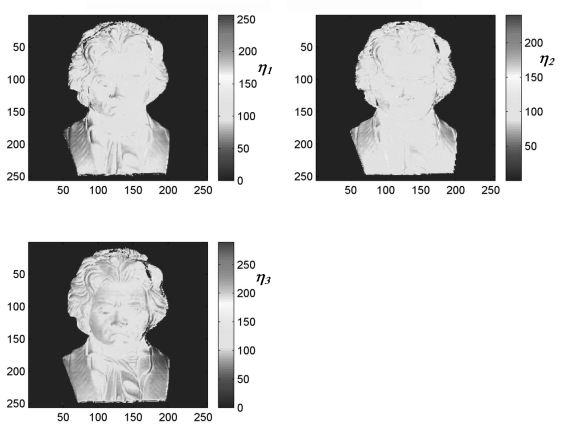

Figure 3: Intensity representation of calculated η values.

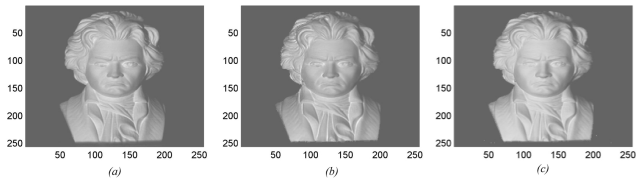

Figure 4: (a) is the original image illuminated by ls_1, (b) is the image rendered using calculated η values, and (c) is the image rendered using constant albedo value.

Notice that the η distributions have similar shapes, irrespective of the light source directions. The η distributions are overlapped in the bottom right graph for comparison. It can be seen that the distributions all have peak values at around 100, and with symmetric and similar spread.

The values of η calculated from the different light sources are represented as intensity values in Fig. 3. It can be seen from Fig. 3 that the values of η have similar distributions in the spatial domain as well.

The calculated η maps are used to render images with different light source directions. An image rendered using constant albedo is also provided. The rendered images are compared with the original image to evaluate the effectiveness of η maps. Figure 4 shows the original and resultant rendered images for ls_1.

In Fig. 4, all rendered surfaces are illuminated by parallel light from light source 3. The intensity values of the rendered images have been scaled to match the intensity values of the original image in Fig. 4(a).

The usual approach to surface visualisation by rendering the surface with a constant albedo value, as shown in Fig. 4(c). It is perceptible from the resultant images that the image intensities of the surface rendered using calculated η maps, i.e. Fig. 4 (b), are more similar to that of the original image than the surface rendered with constant albedo (c). Experiments for other light source directions yield similar results.

Table 1 compares surfaces rendered using η values calculated from three different light source directions and surface rendered using constant albedo. The errors are calculated as the sum of intensity absolute error.

From Table 1, for the example in Fig. 4 and light source direction ls_1, we see that the error between intensity values of a surface with η values obtained

ls_i	η error for ls_1	η error for ls_2	η error for ls_3	constant albedo
ls_1	-	181343	231938	831555
ls_2	211847	-	219368	781607
ls_3	220384	174188	-	684020

Table 1: Sum of absolute errors between original surface and rendered surfaces .

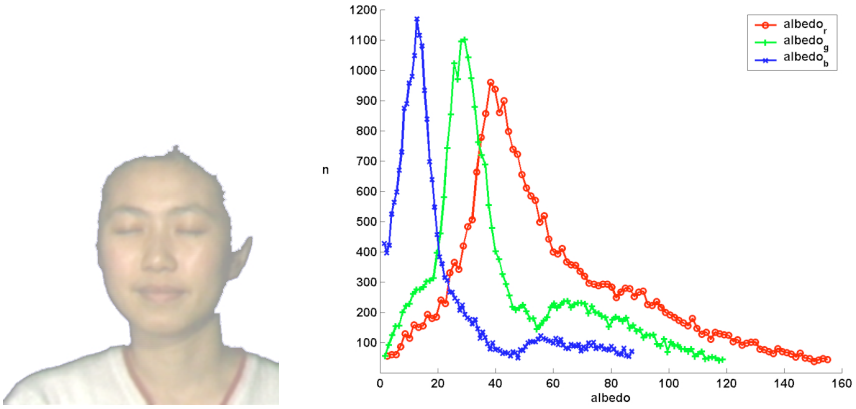

Figure 5: (a)input image for calculation of albedo, and (b)distribution of albedo values for red, green and blue channels.

from ls_1 is 220384 and for ls_2 it is 174188 when the surfaces are rendered using light source direction ls_3. Both errors are much lower than when the surface is rendered using constant albedo, where the error is 684020.

We performed experiments with surfaces having more complex albedo values, such as the human face. The results obtained are shown in Figs. 5 and 6.

From Fig. 6, we can see that the images rendered are consistent with the given light source direction and provide convincing visualisation for the given surface.

The errors in the rendered images for Figs. 4 and 6 may be due to the assumption for $\sigma = 0$. Since in real situation, factors such as interreflection, sensor calibration and the spread of illumination affects the perceived surface reflectance values. In future work, we can take σ into consideration while performing albedo calculations to improve the result of calculated reflectance values.

5 Conclusions

Photometric stereo with colour imaging raises the possiblity that the reflectance function itself can be estimated. Similar work has been carried out by, among others, M. D'Zmura and G. Healy at U. California (Irvine) and coworkers, and D. Greenberg at Cornell and coworkers. However, it would be of interest to build an integrated 3-D scanner which measured both shape and reflectance. We have proposed a method for albedo reconstruction using a photometric stereo approach. In our work, the composite albedo values for a given point on the surface of the object is calculated from the image irradiance and local surface orientations at that point. Experiments have been performed with surfaces

Figure 6: Images rendered using calculated albedos from different light source directions.

with uniform albedo values, such as the plaster bust, and surfaces with complex albedo values, such as the human face. Results have shown that surfaces rendered using the calculated albedo values provide more realistic visualizations than the conventional approach.

6 Acknowledgement

The first two authors wish to thank *Agilent Technologies Laboratories* for supporting this research project.

References

[1] MPEG-4 SNHC Web Home, MPEG-4 Synthetic/Natural Hybrid Coding Development of Media Model Standards, *http://130.187.2.100/mpeg4-snhc/Docs/N1199.html*.

[2] R. Klette, K.Schlüns,Height data from gradient fields, *Proc. SPIE*, 2908, pp.204-215, 1996.

[3] R.J. Woodham: Photometric method for determining surface orientation from multiple images. *Optical Engineering* **19** (1980) 139–144.

[4] M. J. Vrhel, R. Gershon, L. S. Iwan, "Measurement and analysis of object reflectance spectra," *Color research and application*, Vol. 19, No. 1, February 1994, pp 4-9.

[5] Q. Zheng and R. Chellappa, Estimation of illuminant direction, albedo, and shape from shading,*IEEE Trans. on Pattern Analysis and Machine Intelligence*,**PAMI-13** (1991) 680–702.

[6] R. Zhang, P.-S. Tsai,JE Cryer and M. Shah, Shape-from-shading: a survey, *IEEE Trans. on Pattern Analysis and Machine Intelligence*,**PAMI-21** (1999) 690–706.

[7] www.graphics.cornell.edu/online/measurements

[8] www.cvl.uci.edu/overviews/

[9] www.cvr.uci.edu/dzmura/